JCSE The Journal of Corrosion Science and Engineering
ISSN 1466-8858 Volume 15, Preprint 7 submitted 10 January 2012

Electrodeposited Ni-Mo-TiO2 Nanocomposite Coating with High Resistance to Corrosion in Nitric Acid Solution

M.H. Allahyarzadeh[a,b,*], B. Roozbehani[b], A. Ashrafi[c], M. Mohammadi[b]

[a] *Corrosion Department, Iranian Offshore Oil Company, Lavan Island, Iran,*

[b] *Technical Inspection Engineering Department, Abadan Faculty of Petroleum Engineering, Petroleum University of Technology, Abadan, 63165, Iran. Tel.: +989130316100; fax: +98 6314423520.*

[c] *Materials Engineering Department, Faculty of Engineering, Shahid Chamran University, Ahvaz, Iran*

[*] allahyarzadeh.mh@gmail.com

Abstract

Nickel-molybdenum nanocomposite coatings with TiO_2 nanoparticles were electrodeposited potentiostatically in a sulphate-chloride bath containing TiO_2 nanoparticles. The effect of stirring rate on corrosion performance of nanocomposite coatings was studied. The microstructure of electrodeposits was investigated using scanning electron microscopy (SEM) and the corrosion performance of pure Ni-Mo and Ni-Mo-TiO_2 nanocomposite was evaluated using potentiodynamic polarization and electrochemical impedance spectroscopy in 1M nitric acid media. The results showed that the corrosion performance of nanocomposite coatings is related to the stirring rate, and EIS plots demonstrated different corrosion behaviors at different frequencies.

Keywords: electrodeposition, Ni-Mo-TiO_2 nanocomposite, agitation rate, corrosion resistance.

Introduction

Since the surface is the most important part of any engineering component [1], applying a proper coating onto the surface is a method to improve the surface properties [2].

JCSE The Journal of Corrosion Science and Engineering
ISSN 1466-8858 Volume 15, Preprint 7 submitted 10 January 2012

Nickel-molybdenum alloys are resistant to corrosion and wear. They also exhibit low thermal-expansion coefficients, premium hardness and excellent electrocatalytic properties as well [3-5]. The presence of molybdenum in these materials apparently increases their catalytic activity and improves their mechanical properties such as hardness and wear. High electrochemical activity of the Ni-Mo alloys make them widely used in modern electrochemistry related industry [3,4,5].

Ni-Mo alloys can be produced using several methods; Despite of Metallurgical methods which are not very common because of easy oxidation at the crystallization step and high melting temperature of molybdenum, other advanced processing methods are powder metallurgy, mechanical alloying [6,7], spark plasma sintering [8], laser cladding [9] and electrodeposition. For the electrodeposition of the molybdenum alloys with the iron-group metals the citrate-ammonia baths are used in most of the cases [10-12].

During the 1970s and 1980s, several investigations were focused on the need to produce coatings with enhanced mechanical, corrosion and tribological properties. Electrodeposition is an effective method to produce composite coating through the codeposition of metallic, nonmetallic or polymer particles with metal to improve properties such as corrosion resistance, hardness and wear performance [13,14]. While size of codeposited particles has an important effect on the coating characteristics; coating properties improved with decreasing of codeposited particles size. With the development of nanotechnology, nanocomposite coatings have been developed. These coatings have been carried out by electro-codeposition of inert nano-scale particles with metals or alloys [15,16]. The codeposited nanoparticles improve the coatings performance. The nano-sized particles, suspended in the electrolyte by agitation and/or use of surfactants, can be codeposited with the metal. The inclusion of nano-sized particles can give an increased corrosion and micro-hardness resistance, modified growth to form a nanocrystalline metal deposit. [17].

Among nanoparticle which used in reinforcing nanocomposite materials such as such as SiC, WC, Al_2O_3, SiO_2 and AlN, TiO_2 has attracted tremendous interest in research community due to its wide application in engineering materials [18]. However, little attention has been paid to the incorporation of TiO_2 nano-particulates in Ni-Mo matrix; so far no research has been reported on the application of Ni-Mo-TiO_2 nanocomposite coatings applications.

In current research, the electrodeposition technique has been carried out to incorporate TiO_2 nanoparticles in Ni-Mo metallic matrix in order to production of high corrosion resistance Ni-Mo-TiO_2 nanocomposite coatings. The aim of this work is to achieve a high corrosion resistant nanocomposite coating in the nitric acid corrosive media. The effects of

ISSN 1466-8858 Volume 15, Preprint 7 submitted 10 January 2012

bath stirring rate on corrosion resistance of coatings were investigated and corrosion mechanism of nanocomposite coatings in nitric acid was also studied.

Experimentals

Nickel-Molybdenum-TiO_2 nanocomposite coatings were deposited on low carbon steel substrate employing potentiostatic technique. An ammonia-citrate electrolyte was used which its compositions and conditions are presented in Table 1. The solutions were prepared from Merck compounds and distilled water. The pH was adjusted at 9 using ammonium hydroxide or sulfuric acid.

Table 1. Chemical composition of the bath and electrodeposition conditions.

Compositions and conditions	
$NiSO_4.6H_2O$	0.1 M
$NiCl_2.6H_2O$	0.1 M
$Na_2MoO4.2H_2O$	0.03 M
$Na_3C_6H_5O_7.2H_2O$	0.25 M
TiO_2 Nano-particle	25 g L−1
Stirring rate before electrodeposition	500 rpm for 14 hr.
Temperature	30 ± 1
pH	9 ± 0.2

The TiO_2 powder was purchased from Degussa (P-25 anastase) and used without any treatment. The average particle size of the TiO_2 powder used in the experiment was about 25 nm. TiO_2 particles were maintained as suspension state in an electrolytic bath by continuous magnetic stirring at rotating speed of 500 rpm for at least 14 h before deposition. The substrates were ultrasonically cleaned in acetone, dipped in acid (10% hydrochloric acid) and finally washed with distilled water before electrodeposition process.

ISSN 1466-8858 Volume 15, Preprint 7 submitted 10 January 2012

During the codeposition process the bath was stirred by a magnetic stirrer in order to keep the particles dispersed and to investigate the different agitation rate on coating characteristics. The anode was a 316 stainless steel and the bath temperature was maintained at 30°C. The surface morphology of nanocomposite coatings were characterized with scanning electron microscopy (SERON AIS-2100).

Potentiodynamic polarization measurements were carried out in a conventional three electrode cell, containing 1M nitric acid of electrolyte at the temperature of 25°C. Platinum and saturated Ag/AgCl electrodes were used as counter electrode and the reference electrode respectively and coated specimens were used as working electrode. Polarization studies were conducted using computer controlled AutoLab PGSTAT 302N at a scan rate of 1 mV/s from -200 to +700 mV with respect to the open circuit potential (OCP). AutoLab GPES (general purpose electrochemical system) software was used for evaluating the experimental data.

Electrochemical impedance spectroscopy (EIS) measurements were also carried out from 100 kHz to 10 mHz frequency, using computer controlled AutoLab PGSTAT 302N at the temperature of 25 °C in a conventional three electrode cell containing 1M nitric acid solution. The peak-to-peak amplitude of the sinusoidal voltage signal was 10 mV. NOVA 1.6 and Zview softwares were used for evaluating the experimental corrosion data and fitting the equivalent circuit model, respectively.

Results and Discussion

SEM Analysis

Fig. 1 represents the scanning electron microscopy (SEM) micrographs of Ni-Mo-TiO_2 nanocomposite coatings.

Fig. 1a and 1b show low magnification of Ni-Mo-TiO_2 nanocomposite coating. At this figure TiO_2 nanoparticles can be observed in tiny bright regions. But to proof this claim that TiO_2 nanoparticles codeposited into the Ni-Mo matrix in nano-size, greater magnification is required. Fig. 1c and 1d demonstrate nanocomposite coatings in greater scales. Fig. 1d clearly revealed that TiO_2 nanoparticles deposited less than 100 nm.

JCSE The Journal of Corrosion Science and Engineering
ISSN 1466-8858 Volume 15, Preprint 7 submitted 10 January 2012

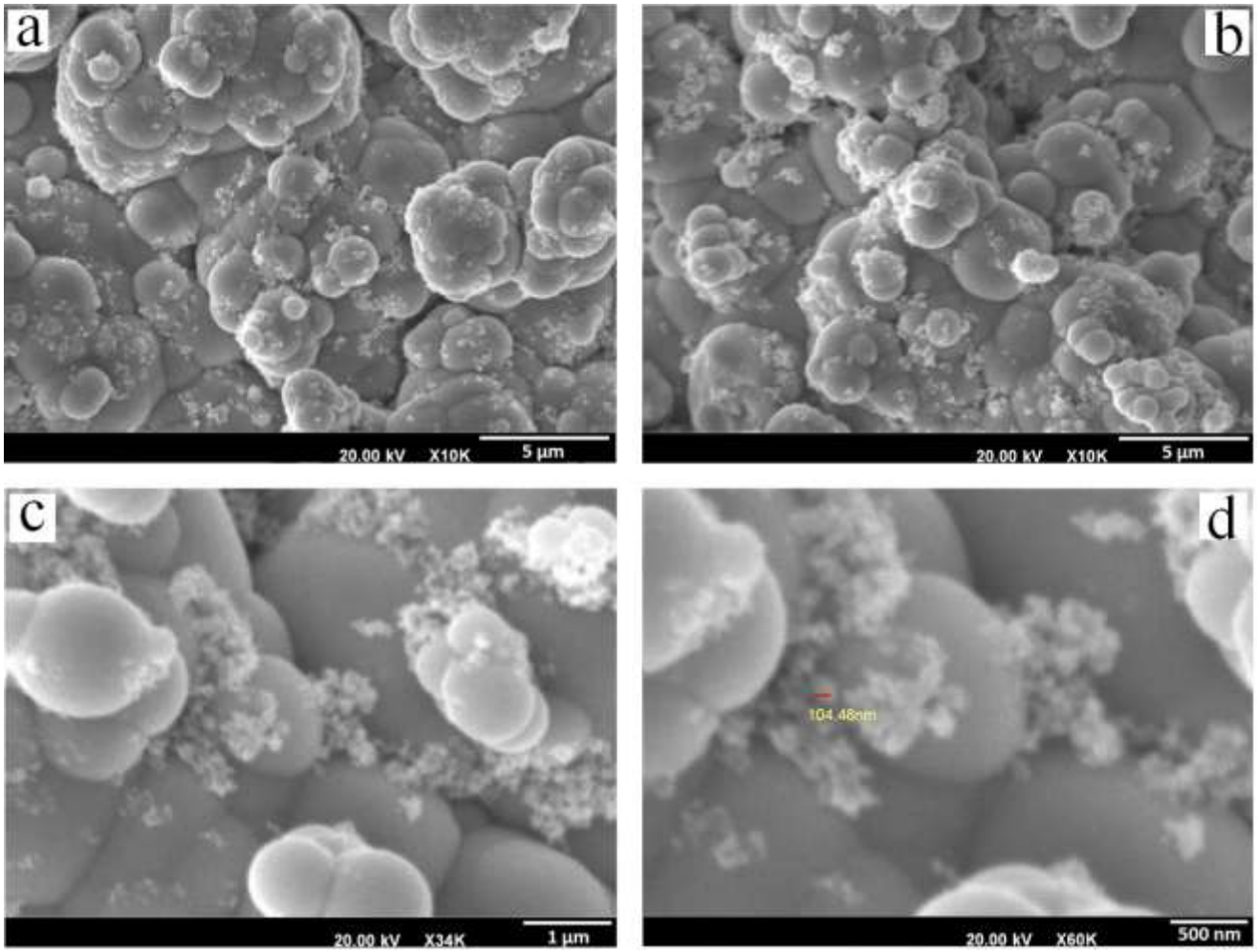

Fig. 1. SEM micrographs of Ni-Mo-TiO2 nanocomposite coatings deposited from citrate-ammoniacal solution.

Corrosion Analysis

The anti-corrosion performance of substrate coated with pure Ni-Mo and Ni-Mo-TiO_2 nanocomposite coating were investigated using potentiodynamic polarization technique and electrochemical impedance spectroscopy (EIS) method in 1M nitric acid solution.

The cyclic potentiodynamic polarization curves of the pure Ni-Mo and nanocomposite coatings with different stirring rates are shown in Fig. 2. The important electrochemical parameters including corrosion potential (E_{corr}), corrosion current density (i_{corr}) and cathodic Tafel slope (β_c) calculated from Tafel plots using GPES (general purpose electrochemical system) software are listed in Table 2. The corrosion rates (rcorr) and polarization resistance (R_p) are also calculated from these data.

JCSE The Journal of Corrosion Science and Engineering
ISSN 1466-8858 Volume 15, Preprint 7 submitted 10 January 2012

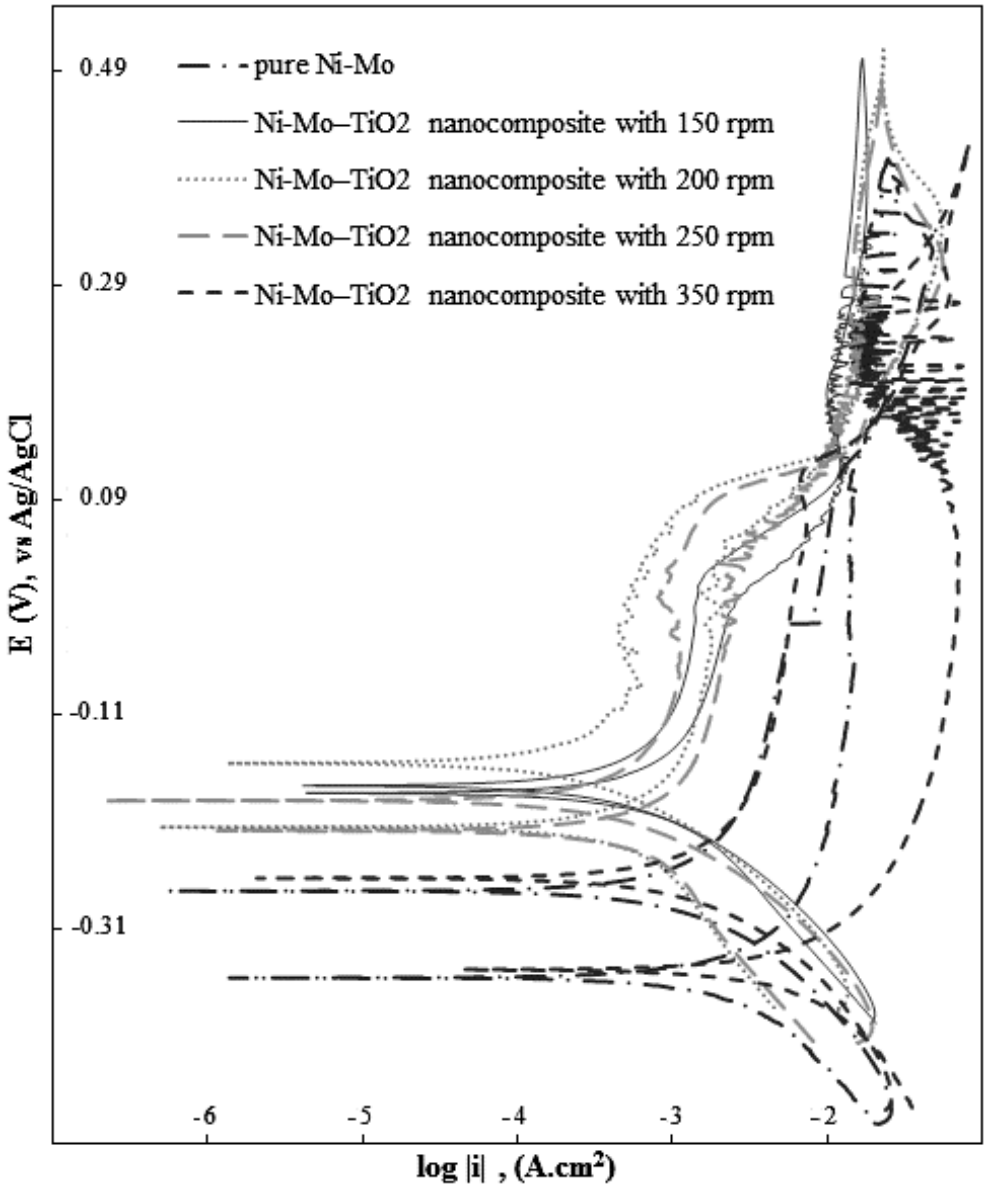

Fig. 2. Cyclic potentiodynamic polarization of pure Ni-Mo and Ni-Mo-TiO2 nanocomposite coatings in 1M nitric acid aqueous solution.

It should be noted that, for determination of corrosion rates and polarization resistances just cathodic Tafel slope was used; anodic and cathodic Tafel slopes considered being the same.

From the Table 2, it is obvious that by increasing the stirring rate, at first the corrosion current density decreases and then increases after 200 rpm. Also it is clear that nanocomposite coatings have better anti-corrosion properties rather than pure Ni-Mo.

JCSE The Journal of Corrosion Science and Engineering
ISSN 1466-8858 Volume 15, Preprint 7 submitted 10 January 2012

Table 2. Electrochemical parameters obtained from the Tafel plots for bare metal, pure Ni-Mo and Ni-Mo-TiO_2 nanocomposite

Sample	TiO_2 Wt.%	E_{corr} (mv)	βc (mv/dec)	i_{corr} (mA/cm2)	R_p (Ω/cm2)	r_{corr} (mpy)
Bare Metal	-	-303	584	73.53	1.727	7.29×102
Pure Ni-Mo coating	-	-274	167	1.57	23.12	18.51
Ni-Mo-TiO2 with 150rpm	5±.5	-176	136	1.065	27.76	10.56
Ni-Mo-TiO2 with 200rpm	8±.5	-155	123	0.516	51.82	5.11
Ni-Mo-TiO2 with 250rpm	6±.5	-190	123	1.03	25.96	10.21
Ni-Mo-TiO2 with 350rpm	3±.5	-262	158	3.16	10.87	37.2

Fig. 3A shows the relation between stirring rate of the bath and corrosion current density. As shown in this figure, at 200 rpm the minimum corrosion current density and consequently the best corrosion resistance has obtained. Exactly the same behavior has seen for open circuit potential of coatings. As represented in Fig. 3B the noblest potential was related to the stirring rate of 200 rpm too. P. Baghery et al. [19] reported such relation between stirring rate and the amount of TiO_2 nanoparticle embedded in the Ni matrix. They reported the stirring rate strongly affects the concentration (wt.%) of TiO_2 nanoparticles.

Their experimental results in 1M nitric acid solution showed at 180 rpm stirring rate the best corrosion performance was obtained. As illustrated in Fig. 3A and Fig. 3B increasing rotation rate over 200 rpm has decreased the corrosion performance of the deposits. It is concluded that the amount of TiO_2 nanoparticles codeposited into the Ni-Mo matrix directly relates to the stirring rate of solution. The presence of TiO_2 nanoparticle has clearly enhanced the corrosion resistance of Ni-Mo coatings.

For investigating the corrosion mechanism and corrosion behaviour of the coatings in nitric acid solution, electrochemical impedance spectroscopies were also carried out. Fig. 4 demonstrates the Nyquist and Bode plots of coatings in 1 M nitric acid solution respectively.

JCSE The Journal of Corrosion Science and Engineering
ISSN 1466-8858 Volume 15, Preprint 7 submitted 10 January 2012

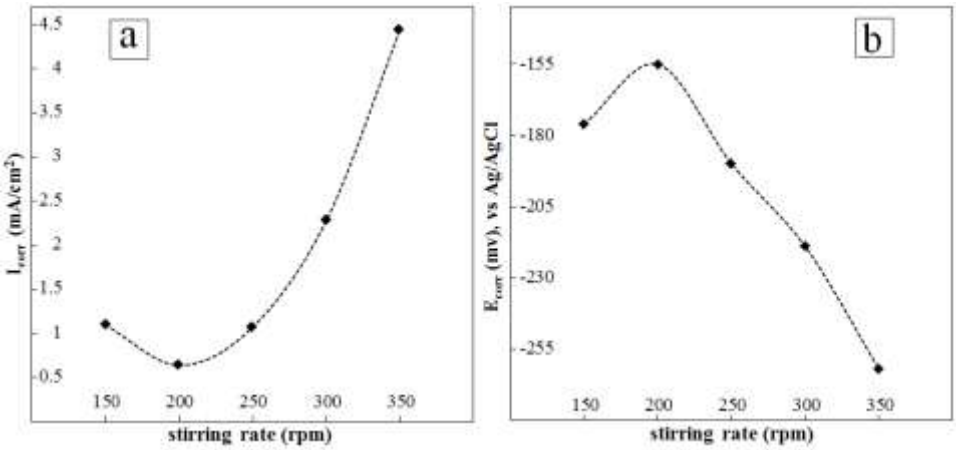

Fig. 3. Effect of stirring rate on corrosion current density (a) and open circuit potential (b) of Ni-Mo- TiO_2 nanocomposite coatings.

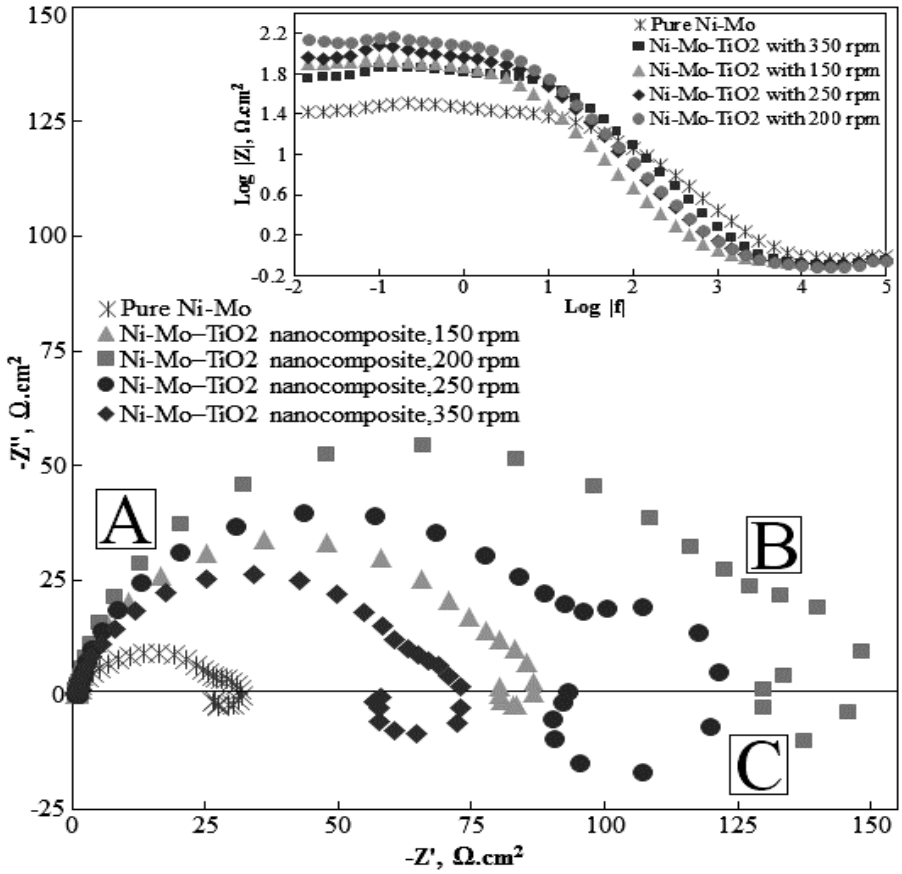

Fig. 4. Nyquist and Bode plots of pure Ni-Mo and Ni-Mo-TiO_2 nanocomposite coatings in 1M nitric acid.

JCSE The Journal of Corrosion Science and Engineering
ISSN 1466-8858 Volume 15, Preprint 7 submitted 10 January 2012

In Nyquist plots, the intersection points between the inductive loop and capacitive loop with the real axis approximately present (R_s+R_{ct}) and R_s respectively. All the Nyquist diagrams illustrate one depressed capacitive loop at the higher frequencies (HF) which is followed by an inductive loop (position C in Fig. 4) that can be observed in the lower frequencies (LF). The capacitive loop is attributed to the charge transfer resistance, and the inductive loop can be related to the relaxation processes obtained by adsorbed species like H^{+}_{ads} and NO^{3-}_{ads} on the electrode surface [21]. In other words, the inductive behaviour at low frequencies is probably due to the consequence of the layer stabilization by-products of the corrosion reaction or corrosion products on the electrode surface as a protective layer. According to the literature [20-23], Baril et al. proposed a kinetic model to describe the mechanism of these types of corrosion with such typical impedance spectra. It has been noticed that, medium-frequency capacitive loop suggests diffusion impedance (position B in Fig. 4). As noticed before, inductive loops are generally ascribed to the existence of relaxation processes of adsorbed species [21-23].

According to the this kinetic model; the medium-frequency capacitive loop suggests diffusion impedance, thus this loop can be attributed to diffusion through the porous layer of $M(OH)_2$ (metal hydroxide formed on electrode surface). The presence of the inductive loop in the low-frequency range might involve an adsorbed species; M^+ is assumed to be the absorbed (M^+ is the simplest species which can be involved in the coating corrosion as an intermediate). The high-frequency capacitive loop corresponds to the charge transfer resistance of Reactions 1 and 2, (position A in Fig. 4) on the film area, the two reactions considered are:

$$M \xrightarrow{k1} (M^+)_{ads} + e^- \qquad (1)$$

and

$$(M^+)_{ads} \xleftrightarrow{k2} M^{2+} + e^- \qquad (2)$$

a chemical reaction was also introduced as follow:

$$(M^+)_{ads} + H_2O \xrightarrow{k3} M^{2+} + OH^- + \frac{1}{2} H_2 \qquad (3)$$

The mass transport loop (position B in Fig. 4) in the medium-frequency range corresponds to the diffusion of M^{2+} through the porous $M(OH)_2$ layer (metal hydroxide); therefore, M^{2+}

JCSE The Journal of Corrosion Science and Engineering
ISSN 1466-8858 Volume 15, Preprint 7 submitted 10 January 2012

reacts at the interface. The formation of MO layer (metal oxide) corresponds to the following equilibriums:

$$M^{2+} + 2OH^- \xleftrightarrow{k4} M(OH)_2 \quad (4)$$

$$M(OH)_2 \xleftrightarrow{k5} MO + H_2O \quad (5)$$ corrosion product formation

It is reported that, this layer is homogeneous and covers the entire coating surface [29]. Hence, it can be assumed that active zones (without metal oxide) are moving on the coating surface. Strictly speaking, active zones become passive, and new active zones are created near the passive ones. If the presence of the active zones attributes to localized corrosion, it is not highly localized corrosion, such as pitting corrosion for aluminum and aluminum alloys.

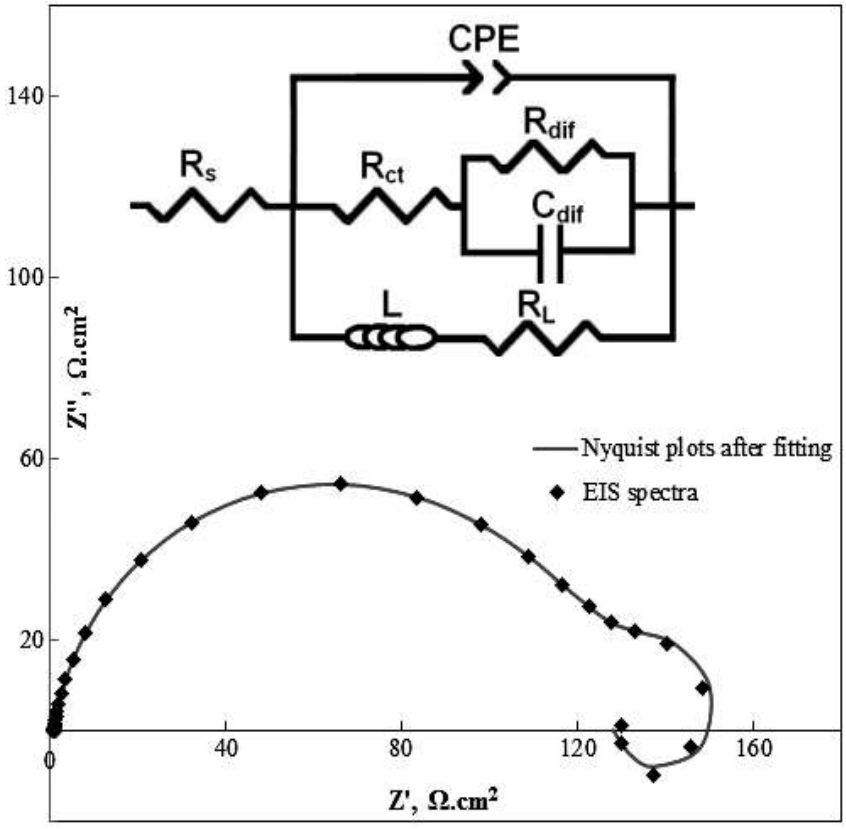

Fig. 5. Equivalent circuit for EIS plots of coatings in 1M nitric acid solution and Nyquist plot after fitting EIS for Ni-Mo-TiO_2 nanocomposite coatings with 200 rpm stirring rate.

JCSE The Journal of Corrosion Science and Engineering
ISSN 1466-8858 Volume 15, Preprint 7 submitted 10 January 2012

The equivalent circuit model which is fitted to this corrosion mechanism is shown in Fig. 5. The equivalent circuit models were fitted by Zview software; the model represents reasonable and sound fit with EIS plots for both Ni-Mo and Ni-Mo-TiO_2 nanocomposite coatings. Fig. 5 represents also Nyquist plot after fitting EIS spectra fitted for Ni-Mo-TiO_2 nanocomposite coatings, obtained with stirring rate of 200 rpm. This figure demonstrates that, reasonable fitting is obtained by proposed electrochemical circuit model; continuous line represents the results after fitting and also the solid points are related to EIS plot. L and Rl represent the inductance and inductance resistances respectively; C_{dif} and R_{dif} are related to mass transport loop. R_s and R_{ct} also represent solution and charge transfer resistance. Table 3 exhibits that the maximum charge transfer resistance and also maximum resistance against diffusion and mass transport process has related to nanocomposite coatings which were conducted with 200 rpm stirring rate. Moreover the inductor raised from adsorption effects of the oxide film can be defined as ($L=R_\tau$) where τ is the relaxation time for adsorption on electrode surface [20]. The fitting results of EIS plots in nitric acid solution are listed in Table 3.

Table 3. Fitting results of EIS plots for Ni-Mo and Ni-Mo-TiO_2 nanocomposite coatings in 1M nitric acid solution

Sample	TiO_2 Wt.%	R_s (Ω)	R_{ct} (Ω)	R_{dif} (Ω)	R_L (Ω)	CPE (mF.cm-2)	n	C_{dif} (mF.cm-2)	L H.cm2
Pure Ni-Mo with 200 rpm	-	0.7	21.1	3.9	109.4	0.52	0.79	29.40	424.6
Ni-Mo-TiO2 with 150 rpm	5±.5	0.7	62.6	109.1	108.9	0.92	0.88	0.16	0.82
Ni-Mo-TiO2 with 200 rpm	8±.5	0.6	103.7	261.7	143.8	0.45	0.90	12.38	194
Ni-Mo-TiO2 with 250 rpm	6±.5	0.65	76.9	168.5	105.5	0.51	0.89	14.52	167.7
Ni-Mo-TiO2 with 350 rpm	3±.5	0.6	51.2	11.8	155.6	0.33	0.88	36.67	410.3

It is clear that, increasing the stirring rate causes different amount of TiO_2 nanoparticle content in coating and leading to increase the charge transfer resistance. Hence at stirring rate of 200 rpm, the maximum charge transfer resistance has obtained. So the maximum corrosion resistance property of Ni-Mo-TiO_2 nanocomposite coatings in acid nitric solution is obtained at this stirring rate. Both cyclic potentiodynamic polarization and electrochemical impedance spectroscopy have confirmed these results. Considering

literature [19], the results also revealed that corrosion resistance of Ni-Mo-TiO_2 nanocomposite in nitric acid environments is greater than Ni-TiO_2 nanocomposite. By comparison between the literatures [19] and the results in current research, it can be concluded that the Ni-Mo-TiO_2 nanocomposite coatings are much more corrosion resistant than Ni-TiO_2 nanocomposite.

Conclusions

Ni-Mo-TiO_2 nanocomposite coating was deposited by potentiostatic electrodeposition technique. As shown the results one of the important parameters in nano/micro composite coating deposition is solution agitation. Electrochemical impedance spectra and cyclic potentiodynamic polarization showed that the presence of TiO_2 nanoparticles in Ni-Mo matrix coating enhances the corrosion resistance properties of the coatings in nitric acid solution. The EIS spectra demonstrate that corrosion can be controlled by the presence of a very thin oxide film, and the inductive behavior at low frequencies is due to the formation of this oxide film. Also at present conditions the best corrosion resistance was obtained at 200 rpm stirring rate.

Acknowledgment

The authors would like to appreciate the National Iranian Oil Company (NIOC) and research and development department at Iranian Offshore Oil Company (IOOC) for their financial supports. And also they would like to acknowledge the technical staff at the Petroleum University of Technology. We also appreciate Mr. Bahrami, Mr. Nasibi and Mr. Kheradmand for their assistance.

References

[1] 'Wear maps for titanium nitride coatings deposited on copper and brass with electroless nickel interlayers ', C. Subramanian, G. Cavallaro, G. Winkelman, *Wear*, 241, pp228-233, 2000.

[2] 'A review of surface engineering issues critical to wind turbine performance', N. Dalili, A. Edrisy, R. Carriveau, *Renewable Sustainable Energy Reviews*, 13, pp428–438, 2009.

[3] 'Hydrogen evolving activity on nickel–molybdenum deposits using experimental strategies', C.-C. Hu, C.-Y. Weng, *Journal of Applied Electrochemistry*, 30, pp499-506, 2000.

[4] 'Short communication: A novel cathode for alkaline water electrolysis', W.K. Hu, X.J. Cao, F.P. Wang, Y.S. Zhang, *International Journal of Hydrogen Energy*, 22, pp621-623, 1997.

[5] 'Study of Electrodeposited Nickel-Molybdenum, Nickel-Tungsten, Cobalt-Molybdenum, and Cobalt-Tungsten as Hydrogen Electrodes in Alkaline Water Electrolysis', C. Fan, D.L. Piron, A. Steb, P. Paradis, *Journal of Electrochemical Society*, 141, pp382-387, 1994.

[6] 'Hydrogen evolution on hot and cold consolidated Ni–Mo alloys produced by mechanical alloying', P. Kedzierzawski, D. Oleszak, M. Janik-Czachor, *Materials Science and Engineering A*, 300, pp105-112, 2001.

[7] 'Structure of Mechanically Alloyed Ni-Mo Powders', D. Oleszak, V.K. Portnoy, H. Matyja, *Materials Science Forum*, 312, pp345-350, 1999.

[8] 'Nickel-molybdenum catalysts fabricated by mechanical alloying and spark plasma sintering', S.D. De la Torre, D. Oleszak, A. Kakitsuji, K. Miyamoto, H. Miyamoto, R. Martinezm-S, F. Almeraya-C, A. Martinez-V and D. Rios-J, *Materials Science and Engineering A*, 276, pp226-235, 2000.

[9] 'Laser cladding of Ni-Mo alloys for hardfacing applications', G.L. Goswami, S. Kumar, R. Galun, B.L. Mordike, *Lasers in Engineering*, 13, pp1-8, 2003.

[10] 'A study on pulse plating amorphous Ni-Mo alloy coating used as HER cathode in alkaline medium', Qing Han, Shuang Cui, Nianwen P, Jianshe Chen, Kuiren Liu, Xujun Wei, *International Journal of Hydrogen Energy*, 35, pp5194-5201, 2010.

[11] 'Electrodeposition of Ni–Mo alloy coatings and their characterization as cathodes for hydrogen evolution in sodium hydroxide solution', N.V. Krstajic, V.D. Jovic, Lj. Gajic-Krstajic, B.M. Jovic, A.L. Antozzi and G.N. Martelli, *International Journal of Hydrogen Energy*, 3, pp3676-3687, 2008.

[12] 'Electrodeposition of nickel-molybdenum alloys from ammonium citrate baths containing intermediate valence molybdenum compounds', M. P. Pavlov, N. V. Morozova, V. N. Kudryavtsev, *Protection of Metals*, 43, pp459-464, 2007.

[13] 'Friction and wear properties of the co-deposited Ni–SiC nanocomposite coating', Y. Zhou, H. Zhang, B. Qian, Applied Surface Science, 253, pp8335-8339, 2007.

[14] 'The wear behaviour of electro-codeposited Ni–SiC composites', K.H. Hou, M.D. Ger, L.M. Wang, S.T. Ke, *Wear*, 253, pp994-1003, 2002.

[15] 'Advanced characterisation of nanocomposite coatings', M.A. Baker, *Surface and Coatings Technology*, 201, pp6105-6111, 2007.

[16] 'Corrosion behavior of electroless Ni-P alloy coatings containing tungsten or nano-scattered alumina composite in 3.5% NaCl solution', A.S. Hamdy, M.A. Shoeib, H. Hady, O.F. Salam, *Surface and Coatings Technology*, 202, pp162-171, 2007.

[17] 'Electrodeposition of composite coatings containing nanoparticles in a metal deposit', C.T.J. Low, R.G.A. Wills, F.C. Walsh, *Surface and Coatings Technology*, 201, pp371-383, 2006.

[18] 'Hard and corrosion resistant nanocomposite coating for Al alloy', A. Abdel Aal, *Materials Science and Engineering A*, 474, pp181-187, 2008.

[19] 'Ni–TiO_2 nanocomposite coating with high resistance to corrosion and wear', P. Baghery, M. Farzam, A.B. Mousavi, M. Hosseini, *Surface and Coatings Technology*; 204, pp3804-3810, 2010.

[20] 'Impedance spectra of the anodic dissolution of mild steel in sulfuric acid', P. Li, T.C. Tan and J.Y. Lee, *Corrosion Science*, 38, pp1935-1955, 1996.

[21] G. Baril, G. Galicia, C. Deslouis, N. Pebere, B. Tribollet, and V. Vivier. An Impedance Investigation of the Mechanism of Pure Magnesium Corrosion in Sodium Sulfate Solutions. J Electrochem Soc 2007; 154: C108-C113.

[22] 'Corrosion characterization of Mg–8Li alloy in NaCl solution', Yingwei Song, Dayong Shan, Rongshi Chen, En-Hou Han, *Corrosion Science*, 51, pp1087-1094, 2009.

[23] 'Local and global electrochemical impedances applied to the corrosion behaviour of an AZ91 magnesium alloy', Gonzalo Galicia, Nadine Pebere, Bernard Tribollet, Vincent Vivier, *Corrosion Science*, 51, pp1789-1794, 2009.